

***Supplemental Material for***  
***Gene function prediction from congruent synthetic lethal***  
***interactions in yeast***

Ping Ye, Brian D. Peyser, Xuewen Pan, Jef D. Boeke, Forrest A. Spencer  
and  
Joel S. Bader

## Synthetic lethal genes bridge parallel pathways

Protein complexes are often the functional units that implement biological processes. Knowledge of protein complex organization can help explain the functions of genes within the context of biological pathways. We hypothesized that protein complex data can reveal quantitative, hierarchical organization of synthetic lethal interactions. Specifically, members of different protein complexes in parallel pathways should cluster in groups of direct synthetic lethal partners. Synthetic lethal interactions between these groups should ‘bridge’ the parallel pathway branches they reveal.

To explore this hypothesis, we first calculated the total number of synthetic lethal interactions between protein complexes using synthetic lethal dataset generated from the SGA approach(Tong et al, 2004) and high-throughput protein complex datasets(Gavin et al, 2002; Ho et al, 2002). Of 3799 synthetic lethal pairs of knock-out mutants, 1083 (~30%) bridge distinct protein complexes, with one member of a synthetic lethal pair in a different complex than its partner. Since only ~1% of synthetic lethal pairs reside within the same protein complex(Tong et al, 2004), a synthetic lethal interaction is 30x more likely to bridge two distinct complexes than reside within a single complex. Analysis using interactions from curated protein complex data(Mewes et al, 2004) and from high-throughput yeast two-hybrid screens(Ito et al, 2001; Uetz et al, 2000) also support our hypothesis that synthetic lethal pairs are more likely to encode proteins without direct physical interactions. A recent computational study reports similar results(Wong et al, 2004).

For each pair of protein complexes reported in large-scale screens(Gavin et al, 2002; Ho et al, 2002), enrichment of synthetic lethal interaction was quantified as the parallel complex score calculated as the negative  $\log_{10}$  of the binominal p-value for number of synthetic lethal interactions observed between members of the two complexes given the overall frequency of synthetic lethal interactions observed in the whole data set (see the next section for detail). Significant numbers of protein complex pairs are observed being bridged by synthetic lethal interactions using the actual synthetic lethal

interactions compared to a randomized set when parallel complex scores  $\geq 3$  (p-value  $< 10^{-5}$ , Fig. S1A). The hierarchical view of synthetic lethal interaction by clustering gene products into protein complexes shows protein complex nodes connected by highly significant parallel complex linkages (Fig. S1B). Analysis using the curated MIPS protein complex dataset (Mewes et al, 2004) generates similar results (Fig. S2).

The *PAC10* complex is the hub of the parallel complex network, with links to 34 other protein complexes (Fig. S1B). Its hub character is due in part to the bias that all four complex components, *PAC10*, *GIM3*, *GIM5*, and *YKE2* (Gavin et al, 2002), are SGA query genes (Tong et al, 2004). The *PAC10* complex proteins detected by mass spectrometry belong to the biochemically characterized Prefoldin complex (*PAC10*, *GIM3*, *GIM4*, *GIM5*, *YKE2*, *PFD1*), involved in tubulin folding and delivering unfolded proteins to cytosolic chaperonin (Geissler et al, 1998; Vainberg et al, 1998). Deletion mutants of Prefoldin complex components are viable, and sensitive to the microtubule-depolymerizing drug benomyl (Geissler et al, 1998). The 34 protein complexes linked with the *PAC10* complex carry out diverse biological processes including cytoskeleton organization and biogenesis, budding, transcription regulation, translational membrane targeting, rRNA processing, and DNA damage response (Ashburner et al, 2000). The synthetic lethal interaction linkages indicate that these pairs of protein complexes provide related, but distinct, cellular functions. For some linkages, the relationship is readily understood given current knowledge. For example, the *PAC10* complex exhibits enhanced synthetic lethal interactions with the *IML3* complex (*IML3*, *MCM21*, *MCM22*, *CTF3*, *CTF19*, *CHL4*, *AME1*, *NKP1*) (Fig. S1B), which is a kinetochore component. It is reasonable to propose that activities of these two protein complexes may be complementary during kinetochore capture or during chromosome movement, when microtubule dynamics and kinetochore activity are coupled. Synthetic lethality may be explained by higher-order effects of combined perturbations of microtubules and kinetochores.

### **Probability of synthetic lethal interaction and parallel complex score**

The probability of at least  $k$  synthetic lethal interactions bridging two protein complexes was calculated from the binomial distribution:

$$p(x \geq k) = \sum_{x=k}^n C(n, x) P^x (1-P)^{n-x},$$

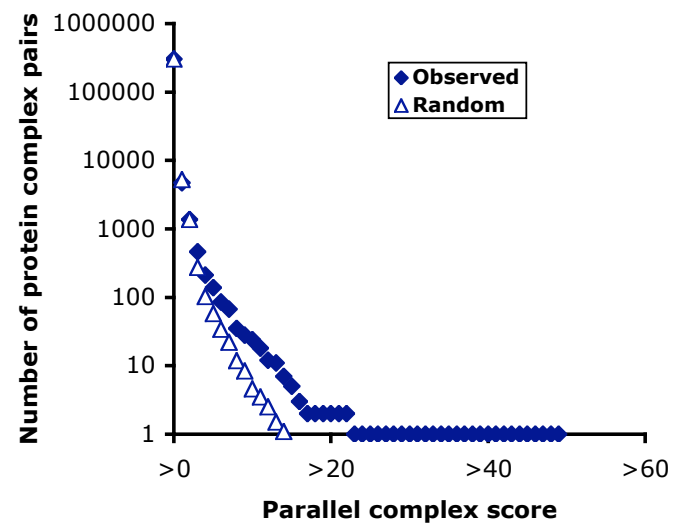
in which  $C(n, x)$  is the combinatorial factor  $n!/x!(n-x)!$ ;  $n$  is the total number of possible interactions between two protein complexes; and  $k$  is the number of observed synthetic lethal interactions between two protein complexes. The probability of observing a set of synthetic lethal interactions between two protein complexes  $P$  was approximated to be 0.0064 from  $a/bc$ , where  $b$  equals 126, the number of query genes,  $c$  equals 4700, the number of target genes, and  $a$  equals 3799, the number of total synthetic lethal interactions observed between query and target genes. The parallel complex score is  $-\log_{10}[p(x \geq k_{\text{obs}})]$ .

We reasoned that for a final p-value of 0.01, an appropriate single-test p-value that incorporates multiple testing all pairs of 780 protein complexes used would be  $\sim 0.01/780^2 = 2 \times 10^{-8}$ , corresponding to a parallel complex score of 7 to 8. As the number of complex pairs nearly doubles when the parallel complex score decreases from 8 to 7 (Fig. S1A), we used 8 as the threshold for the visualization (Fig. S1B). Similarly, threshold 7 was used for Fig. S2B.

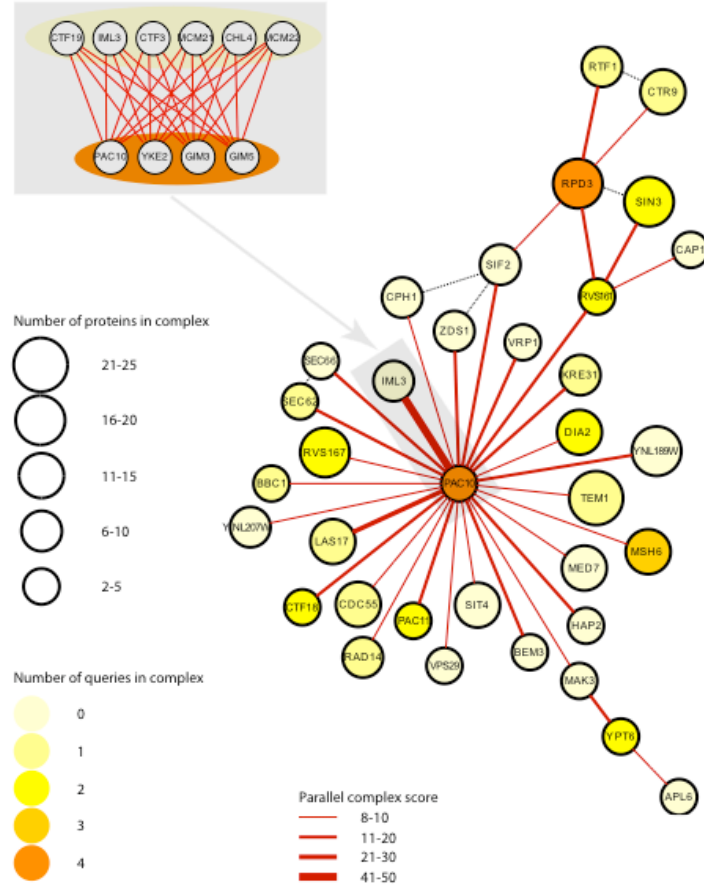
### **Protein complex pair sharing protein components**

The Jaccard coefficient  $c = (n1 \cap n2)/(n1 \cup n2)$ , where  $n1$  is the number of proteins in complex 1 and  $n2$  is the number of proteins in complex 2, was calculated to define comparable protein complexes. The value of 0.4 was used as the threshold of Jaccard coefficient to define similar complexes in Fig. S1B.

A

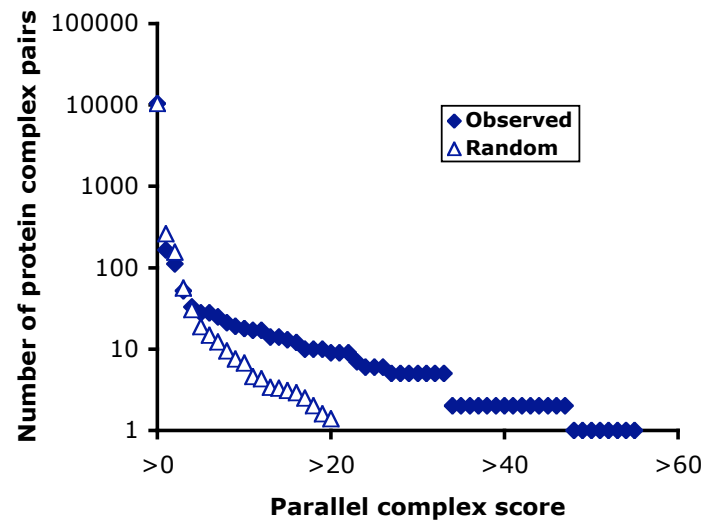


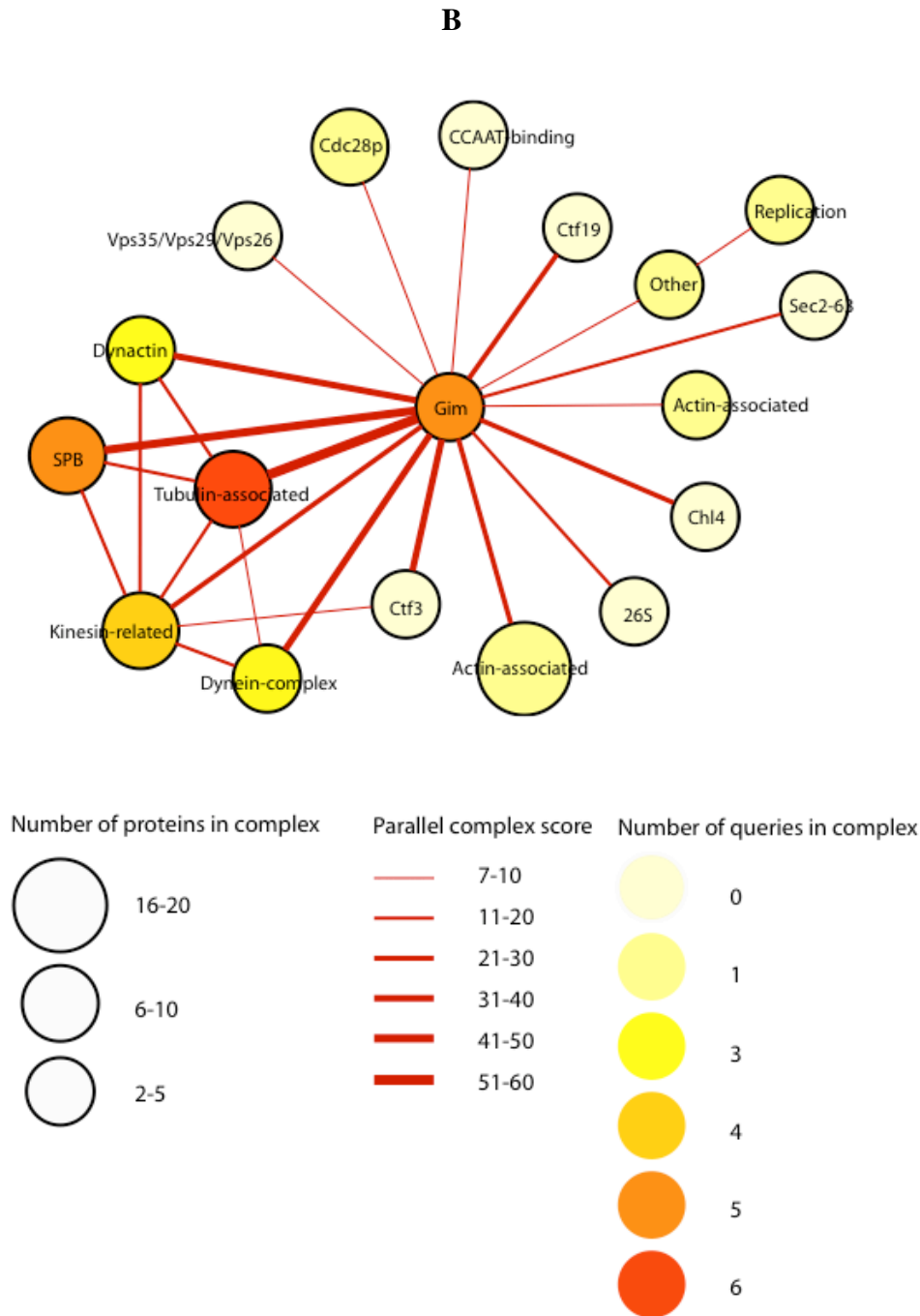
**B**



**Fig. S1.** Synthetic lethal genes bridge parallel pathways from analysis on high throughput protein complex dataset (Gavin et al, 2002; Ho et al, 2002). **(A)** Significant numbers of protein complexes are bridged by synthetic lethal interactions than expected by chance ( $p\text{-value} < 10^{-5}$  when parallel complex score  $\geq 3$ ). **(B)** Pairwise synthetic lethal interactions have been mapped to the level of protein complexes (circles) using the parallel complex score with threshold value  $\geq 8$  (red lines). The size of a circle indicates the number of proteins in the complex, and its color indicates the number of corresponding genes used as SGA queries. Independently reported protein complexes that share multiple components (Jaccard coefficient  $\geq 0.4$ ) are linked (dashed black lines). The shaded inset depicts the pairwise synthetic lethal interactions between components of the *PAC10* and *IML3* complexes that are summarized by a single parallel complex edge.

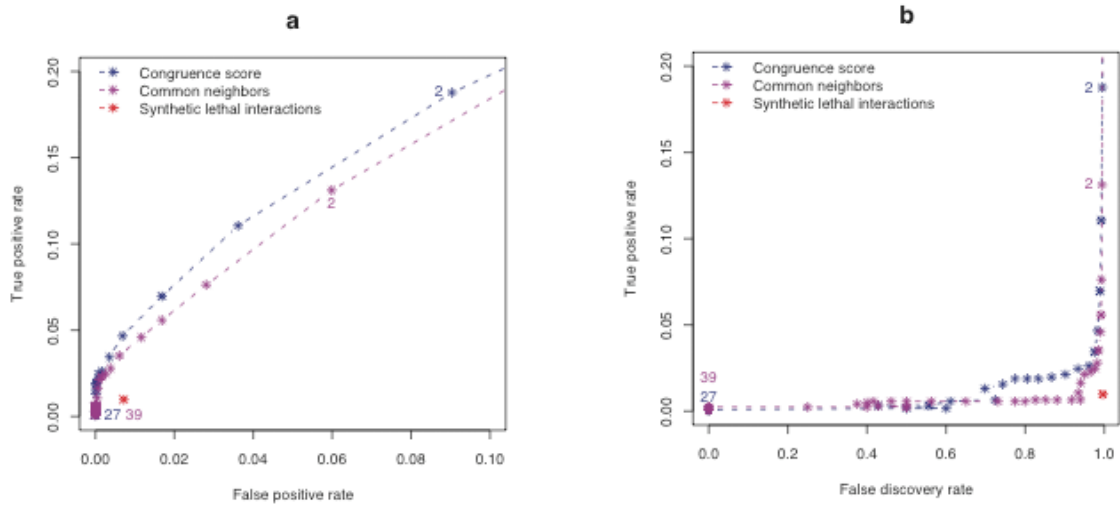
A



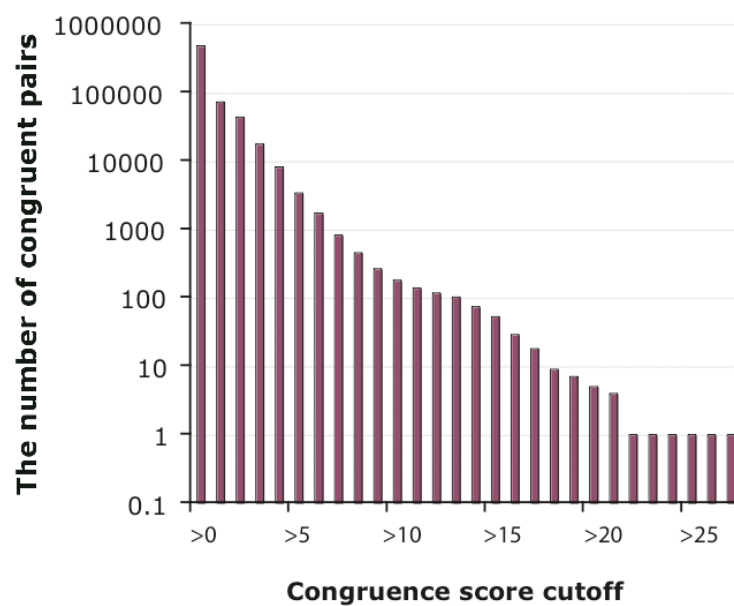


**Fig. S2.** Synthetic lethal genes bridge parallel pathways from analysis on curated MIPS protein complex dataset (Mewes et al, 2004). **(A)** Significant numbers of protein complexes are bridged by synthetic lethal interactions than expected by chance ( $p$ -value  $< 0.001$  when parallel complex score  $\geq 5$ ). **(B)** Pairwise synthetic lethal interactions have been mapped to the level of protein complexes (circles) using the parallel complex score with threshold value  $\geq 7$  (red lines).

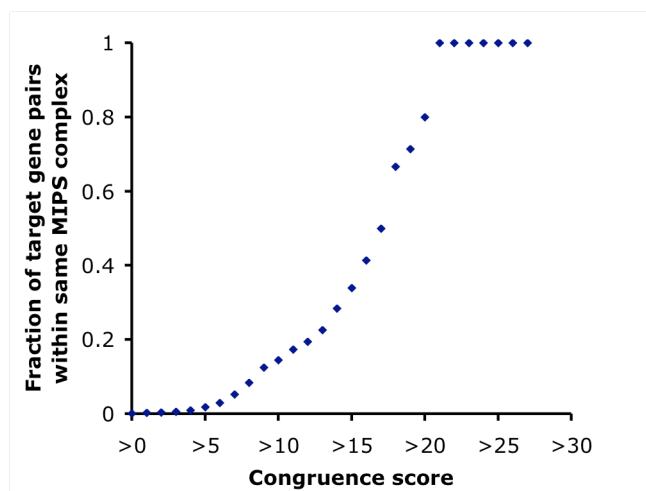




**Fig. S3.** The congruence score method is superior to the number of common neighbors in predicting protein complex coresidence of congruent gene encoded proteins. Prediction of coresidence is presented as a receiver operating characteristic (ROC) curve in terms of the false-positive rate **(A)**, equal to (false positives) / (false positives + true negatives), and the false-discovery rate **(B)**, equal to (false positives) / (false positives + true positives). The numbers indicate the cut-off values for congruence score (blue) and common neighbors (purple). Synthetic lethal interaction (red) has higher false positive rate **(A)** and higher false discovery rate **(B)** in predicting protein complex coresidence as compared with congruence score method when their true positive rates are comparable. The higher ordinate for the congruence score method implies superior performance based on the area under the curve criterion.

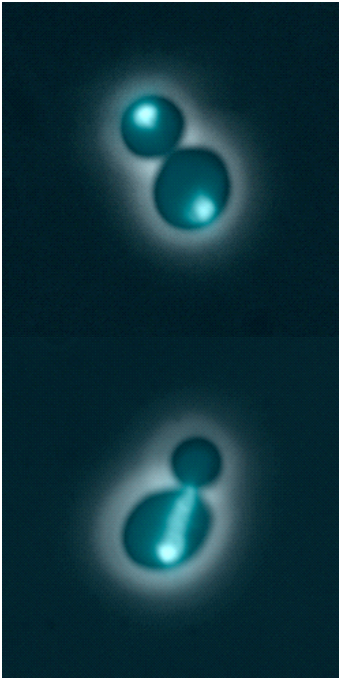


**Fig. S4.** The number of target congruent gene pairs at each congruence score cut-off.

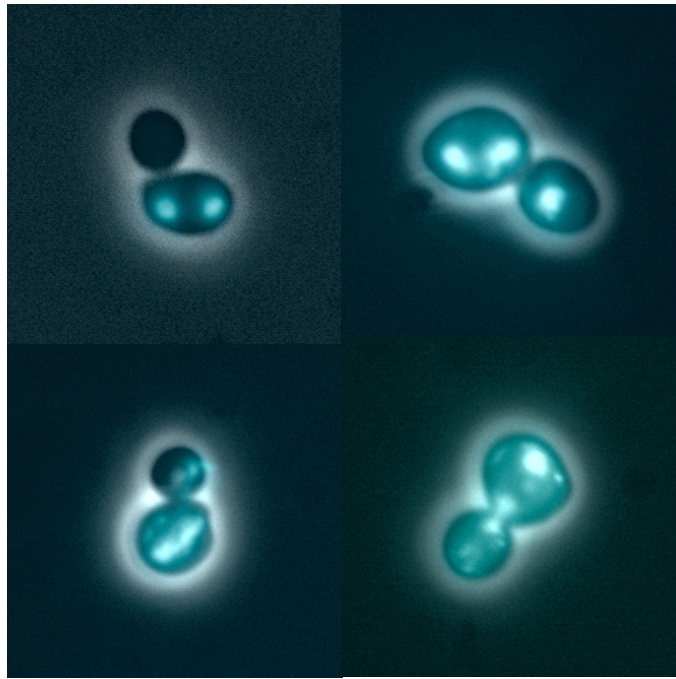


**Fig. S5.** Congruence score predicts protein complex membership using curated MIPS protein complex dataset.

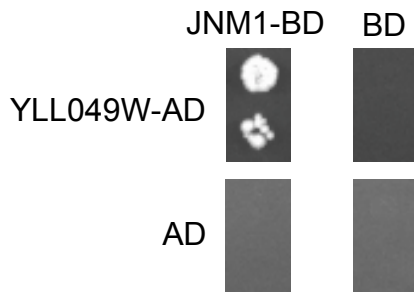
Normal:



Abnormal:



**Fig. S6.** Examples of nuclear migration phenotypes. Left panel, merged Phase/DAPI images of normal nuclear migration events; right panel, merged Phase/DAPI images of abnormal nuclear migration events.



**Fig. S7. Jnm1p binds Yll049wp by yeast-two hybrid assay.**

Yeast-two-hybrid experiments were performed using activation and binding domain vectors pOAD (*LEU2*-marked) and pOBD-2 (*TRP1*-marked), respectively, and yeast strains PJ69-4a and PJ69-4alpha (James et al, 1996). Materials were kindly provided by Stanley Fields, Yeast Resource Center. GAL4-binding domain fusions were transformed into PJ69-4alpha and GAL4-activation domain fusions were transformed into PJ69-4a. The two strains were mated and diploids were selected on SC -Leu -Trp. The resulting diploids were plated on SC -Ade -His media in two dilutions (2  $\mu$ l of 0.1 OD<sub>600</sub>/ml and 0.02 OD<sub>600</sub>/ml) at 30°C. Growth at 4 days is shown.

JNM1-BD, *JNM1* fusion with GAL4 binding domain; YLL049W-AD, *YLL049W* fusion with GAL4 activation domain; BD, binding domain alone; AD, activation domain alone.

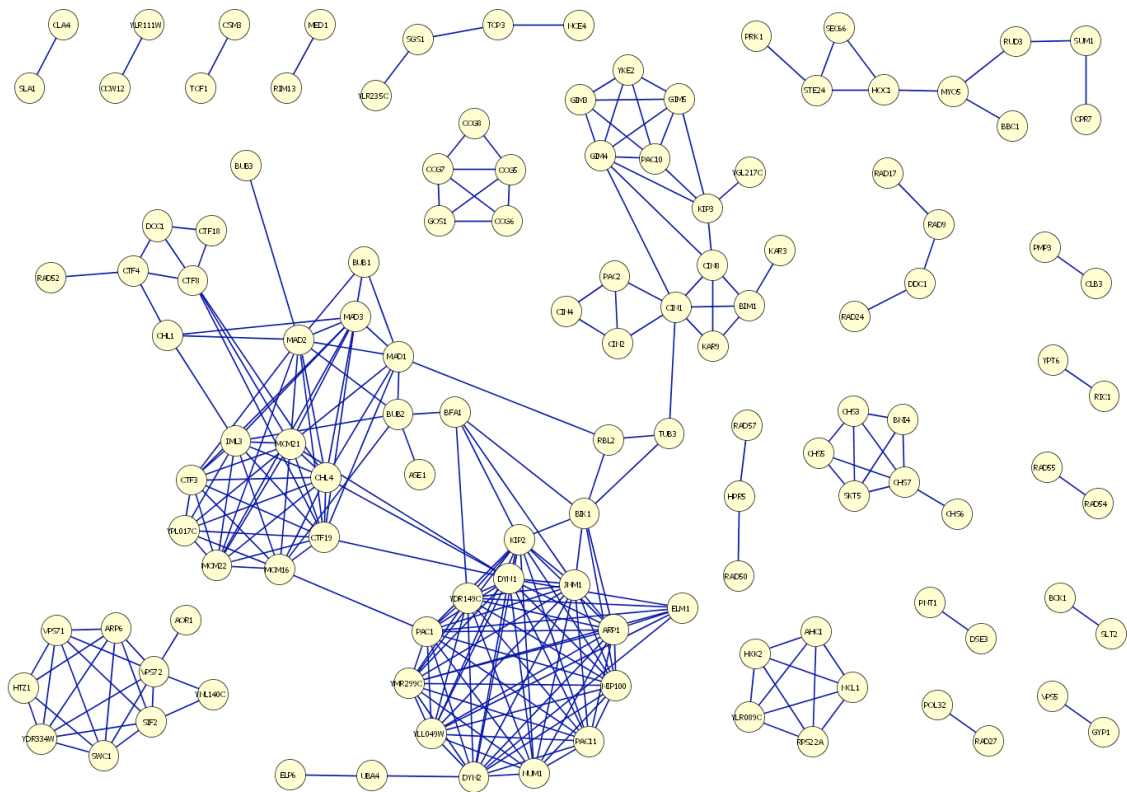
Two independent JNM1-BD and two independent YLL049W-AD transformants supported growth when appropriately combined. YLL049W-BD + AD alone resulted in growth due to self-activation and was therefore not informative (data not shown).

The plasmids and strains used for this study are distinct from those used by Ito, et al (Ito et al, 2001), who reported high-throughput yeast-two-hybrid interaction between *JNM1* and *YLL049W*.

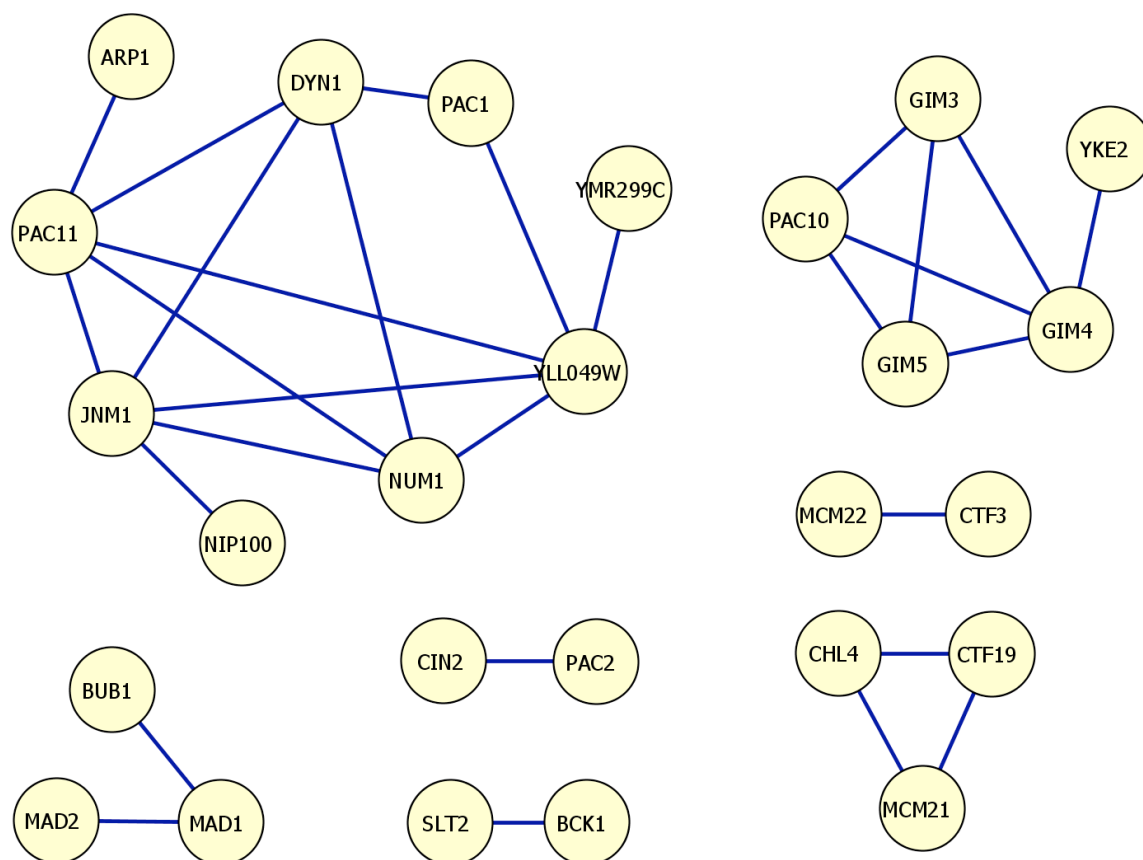
Genotypes:

PJ69-4a: *MATa trp1-901 leu2-3,112 ura3-52 his3-200 gal4Δ gal80Δ LYS2::GAL1-HIS3 GAL2-ADE2 met2::GAL7-lacZ*

PJ69-4alpha: *MATalpha trp1-901 leu2-3,112 ura3-52 his3-200 gal4Δ gal80Δ LYS2::GAL1-HIS3 GAL2-ADE2 met2::GAL7-lacZ*

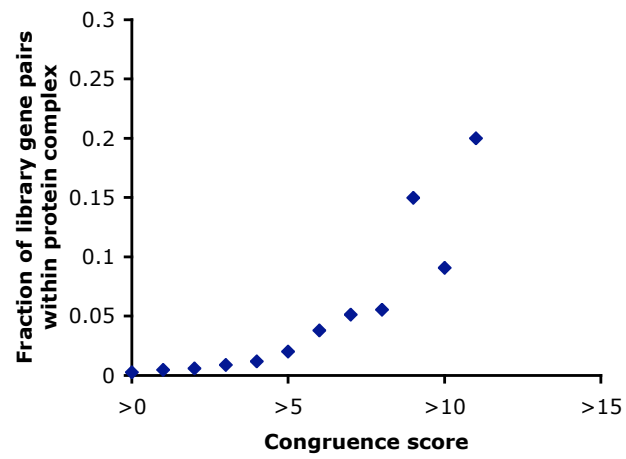


**Fig. S8.** Target gene pair congruence network with the congruence score cutoff greater than or equal to 8.

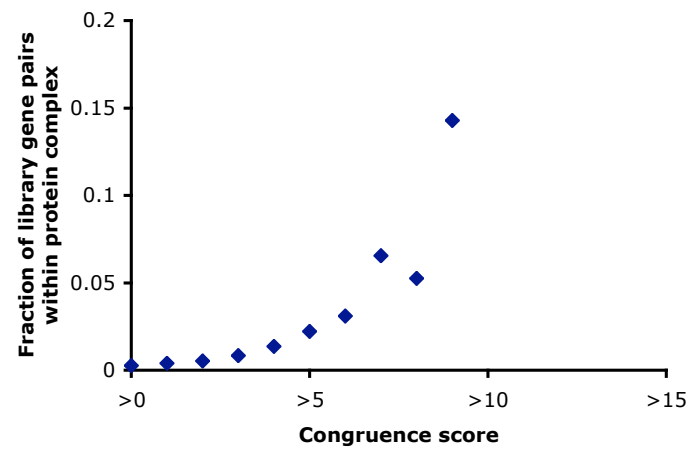


**Fig. S9.** Target gene pair congruence network with the congruence score cutoff greater than or equal to 15.

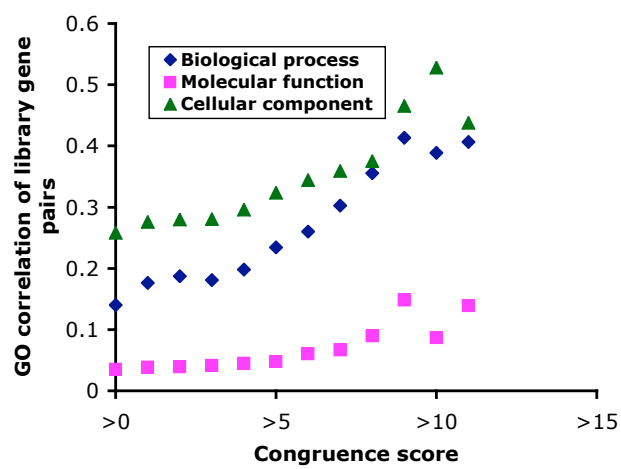
**A**



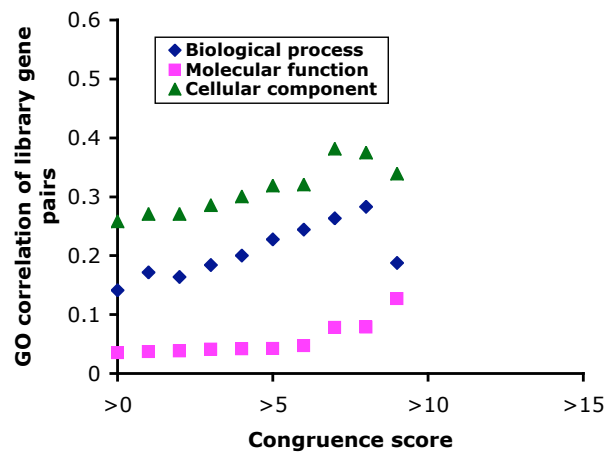
**B**



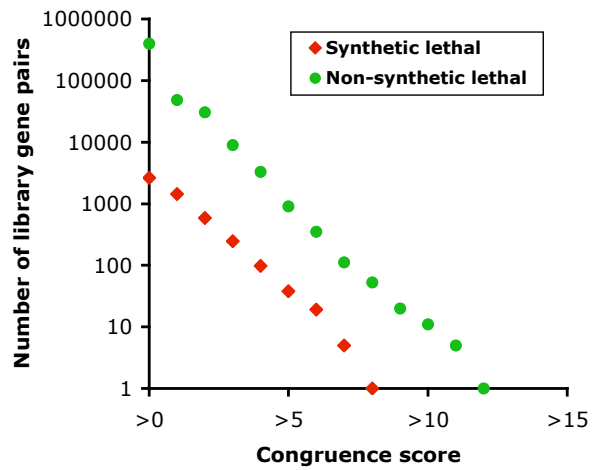
**C**



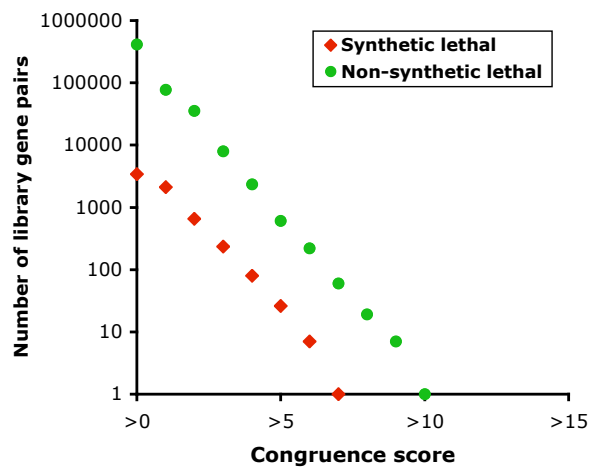
D



E

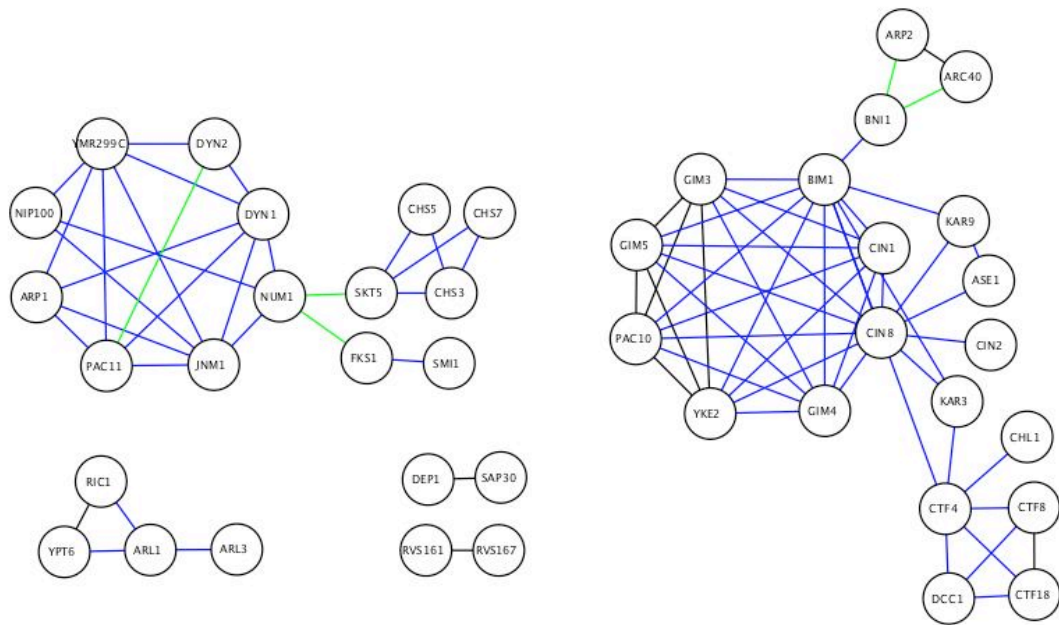


F

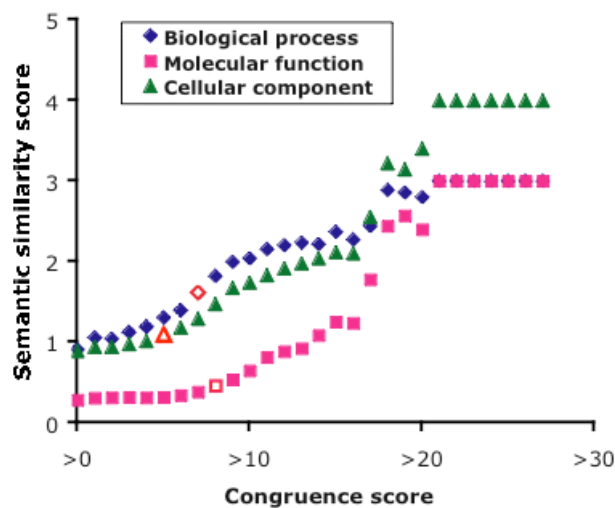




**Fig. S10.** Noise robustness analysis for the congruence method. **(A)**, **(C)**, and **(E)** are results derived from the dataset containing 30% of false negative synthetic lethal interactions. **(B)**, **(D)**, and **(F)** are results derived from the dataset containing 30% of false positive synthetic lethal interactions. The congruence scores generated from datasets containing false negatives and false positives are in the range of 0 to 10 and show similar results as those using the original dataset (compare with Fig. 2a, 2b, 2c). **(A)** and **(B)** A high congruence score predicts protein complex membership. Above congruence score of 3, significant numbers of congruence gene products reside in the same complex as compared with synthetic lethal gene products ( $P < 0.05$ ). **(C)** and **(D)** A high congruence score predicts Gene Ontology (GO) annotation correlations (biological process, molecular function, and cellular component). Above congruence score of (7, 6, 5) and (8, 7, 5) for (c) and (d), respectively, congruence pairs have significantly higher GO correlation (biological process, molecular function, cellular component) as compared with that of synthetic lethal gene pairs ( $P < 0.05$ ). **(E)** and **(F)** High congruence excludes synthetic lethal interaction. Above congruence score of 8 and 7 for (E) and (F), respectively, the binominal p-value for observed number of synthetic lethal interactions is insignificant ( $P > 0.05$ ).



**Fig. S11.** Query gene pair genetic congruence network with the congruence score cutoff greater than or equal to 33. Congruent interactions are labeled with blue lines, physical interactions derived from any two proteins in the same protein complex are labeled with green lines, and black lines represent coexistent congruent and physical interactions.



**Fig. S12. Semantic similarity of congruent genes.**

Semantic similarity(Lord et al, 2003) was calculated for congruent gene pairs and synthetic lethal gene pairs using all yeast gene Gene Ontology annotations for training. Open points indicated the congruence scores at which the semantic similarity for congruent genes rises above similarity for synthetic lethal genes (significance  $p < 0.05$ ). These points show that congruence score out-perform direct synthetic lethal interactions at thresholds of 7 (process), 8 (function), and 5 (component). This is superior performance to that indicated in the main text using GO depth correlation, where the crossovers occurred at 7 (process), 10 (function), and 6 (component).

**Table S1.** True positive rate and false positive rate using different threshold values for congruence score method and number of common neighbors in predicting protein complex coresidence.

	Congruence method				Number of common neighbors			
	TP number	FP number	TP rate	FP rate	TP number	FP number	TP rate	FP rate
0	1220	480451	1.0000	1.0000	1220	480451	1.0000	1.0000
1	307	72444	0.2516	0.1508	307	72611	0.2516	0.1511
2	229	43433	0.1877	0.0904	160	28751	0.1311	0.0598
3	135	17388	0.1107	0.0362	93	13502	0.0762	0.0281
4	85	8102	0.0697	0.0169	68	8104	0.0557	0.0169
5	57	3318	0.0467	0.0069	56	5578	0.0459	0.0116
6	42	1687	0.0344	0.0035	43	2924	0.0352	0.0061
7	32	790	0.0262	0.0016	34	1846	0.0279	0.0038
8	30	423	0.0246	0.0009	30	1236	0.0246	0.0026
9	26	238	0.0213	0.0005	28	793	0.0230	0.0017
10	24	156	0.0197	0.0003	26	493	0.0213	0.0010
11	23	115	0.0189	0.0002	20	315	0.0164	0.0007
12	23	95	0.0189	0.0002	13	186	0.0107	0.0004
13	23	79	0.0189	0.0002	8	125	0.0066	0.0003
14	19	55	0.0156	0.0001	8	89	0.0066	0.0002
15	16	37	0.0131	0.0001	8	59	0.0066	0.0001
16	8	21	0.0066	0.0000	8	46	0.0066	0.0001
17	7	11	0.0057	0.0000	8	38	0.0066	0.0001
18	4	5	0.0033	0.0000	7	28	0.0057	0.0001
19	4	3	0.0033	0.0000	7	24	0.0057	0.0000
20	2	3	0.0016	0.0000	7	19	0.0057	0.0000
21	2	2	0.0016	0.0000	7	13	0.0057	0.0000
22	1	0	0.0008	0.0000	7	9	0.0057	0.0000
23	1	0	0.0008	0.0000	7	7	0.0057	0.0000
24	1	0	0.0008	0.0000	7	6	0.0057	0.0000
25	1	0	0.0008	0.0000	7	5	0.0057	0.0000
26	1	0	0.0008	0.0000	6	4	0.0049	0.0000
27	1	0	0.0008	0.0000	5	3	0.0041	0.0000
28	-	-	-	-	4	3	0.0033	0.0000
29	-	-	-	-	3	3	0.0025	0.0000
30	-	-	-	-	3	3	0.0025	0.0000
31	-	-	-	-	3	2	0.0025	0.0000
32	-	-	-	-	3	1	0.0025	0.0000
33	-	-	-	-	3	0	0.0025	0.0000
34	-	-	-	-	3	0	0.0025	0.0000
35	-	-	-	-	3	0	0.0025	0.0000
36	-	-	-	-	1	0	0.0008	0.0000
37	-	-	-	-	1	0	0.0008	0.0000

38	-	-	-	-	1	0	0.0008	0.0000
39	-	-	-	-	1	0	0.0008	0.0000
ROC area	0.555				0.553			
SE	0.00859				0.00858			

**Table S2.** Nuclear migration phenotypes at 13°C. Deletion mutants for each gene were obtained from the yeast deletion collection (Research Genetics).

ORF name	Gene name	Normal	Abnormal	Percent abnormal	Average congruence score	GO slim Biological Process
(BY4741)	(WT)	94	6	6	NA	
YDR488C	PAC11	29	71	71	15.6	cytoskeleton organization and biogenesis
YMR294W	JNM1	38	62	62	14.8	cell cycle
YKR054C	DYN1	51	49	49	14.4	cytoskeleton organization and biogenesis
YDR150W	NUM1	33	67	67	14.3	cytoskeleton organization and biogenesis
YHR129C	ARP1	18	82	82	14.1	cell cycle
YLL049W		42	58	58	13.9	unknown
YOR269W	PAC1	37	63	63	13.2	cytoskeleton organization and biogenesis
YDR424C	DYN2	60	40	40	12.8	cytoskeleton organization and biogenesis
YMR299C		49	51	51	12.8	unknown
YPL155C	KIP2	86	14	14	10.8	cytoskeleton organization and biogenesis
YCL029C	BIK1	31	19	38	8.0	cell cycle
YKL048C	ELM1	48	2	4	7.5	cytokinesis
YJR053W	BFA1	48	2	4	7.3	conjugation
YPL018W	CTF19	48	2	4	7.0	cell cycle
YDR254W	CHL4	48	2	4	7.0	cell cycle
YDR318W	MCM21	48	2	4	7.0	cell cycle
YHR111W	UBA4	49	1	2	6.9	protein modification
YPR046W	MCM16	48	2	4	6.5	cell cycle
YBR107C	IML3	48	2	4	6.4	cell cycle
YMR055C	BUB2	48	2	4	6.2	cell cycle
YMR312W	ELP6	49	1	2	5.9	transcription
YJR135C	MCM22	47	3	6	5.9	cell cycle
YLR381W	CTF3	44	6	12	5.9	cell cycle
YOR058C	ASE1	50	0	0	5.5	cell cycle
YJL030W	MAD2	50	0	0	5.2	cell cycle

YOR265W	RBL2	48	2	4	5.2	protein binding
YLR386W	VAC14	47	3	6	5.1	organelle organization and biogenesis
YCR086W	CSM1	45	5	10	5.1	DNA metabolism
YLR089C		50	0	0	4.9	unknown
YOR023C	AHC1	50	0	0	4.9	DNA metabolism
YBL024W	NCL1	48	2	4	4.9	RNA metabolism
YBL051C	PIN4	48	2	4	4.9	cell cycle
YJL190C	RPS22A	49	1	2	4.9	protein biosynthesis
YER177W	BMH1	45	5	10	4.9	pseudohyphal growth
YML124C	TUB3	49	1	2	4.8	meiosis
YOR264W	DSE3	48	2	4	4.7	unknown
YOR266W	PNT1	48	2	4	4.7	membrane organization and biogenesis
YGL086W	MAD1	49	1	2	4.6	transport
YPL017C		48	2	4	4.6	unknown
YMR078C	CTF18	44	6	12	4.5	cell cycle
YPL008W	CHL1	47	3	6	4.4	cell cycle
YPR023C	EAF3	48	2	4	4.4	protein modification
YMR138W	CIN4	43	7	14	4.2	cytoskeleton organization and biogenesis
YIL095W	PRK1	49	1	2	4.2	cytokinesis
YCL016C	DCC1	48	2	4	4.1	cell cycle
YLR085C	ARP6	43	7	14	4.0	transport
YGR270W	YTA7	50	0	0	3.9	protein catabolism
YLL006W	MMM1	49	1	2	3.9	organelle organization and biogenesis
YLR292C	SEC72	49	1	2	3.9	transport
YKL025C	PAN3	49	1	2	3.9	DNA metabolism
YDR183W	PLP1	49	1	2	3.9	cytoskeleton organization and biogenesis
YOR026W	BUB3	47	3	6	3.8	cell cycle



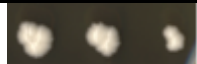
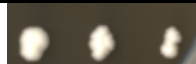

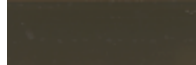

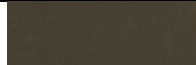
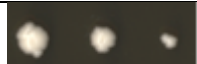
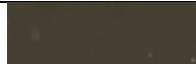
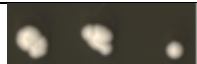
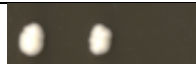
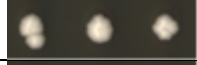
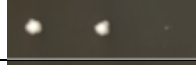
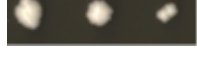
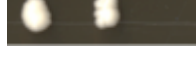
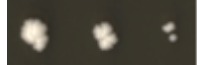

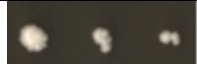

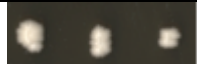
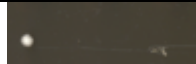
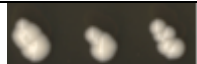
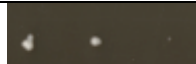
YPR135W	CTF4	49	1	2	3.7	DNA metabolism
YBR103W	SIF2	48	2	4	3.7	meiosis
YFR019W	FAB1	49	1	2	3.7	response to stress
YGR188C	BUB1	47	3	6	3.6	protein modification
YDR485C	VPS72	41	9	18	3.3	transport
YPL253C	VIK1	50	0	0	3.1	cytoskeleton organization and biogenesis
YNL140C		50	0	0	2.8	unknown



**Table S3.** Null mutant of previously uncharacterized yeast ORF *YLL049W* exhibits temperature-dependent nuclear migration defect similar to Dynactin component *JNM1* and distinct from the temperature-independent defect of Kinesin-related gene *KIP2*.

	Mutant	Normal	Abnormal
30°C	<i>BY4741</i> (WT)	97	3
	<i>jnm1Δ</i>	86	14
	<i>kip2Δ</i>	87	13
	<i>yll049wΔ</i>	85	15
13°C	<i>BY4741</i> (WT)	94	6
	<i>jnm1Δ</i>	38	62
	<i>kip2Δ</i>	86	14
	<i>yll049wΔ</i>	42	58

**Table S4.** Benomyl sensitivity at 5ug/ml for mutants congruent to *CIN1*. Approximately equal amounts (OD<sub>600</sub>) of each mutant were arrayed with three five-fold serial dilutions on media with and without 5ug/ml Benomyl in DMSO using a 96-pin transfer device. Mutants were blind scored as Benomyl sensitive if they displayed any decrease in growth compared to DMSO alone.

ORF name	Gene name	Congruence score to CIN1	Ben <sup>S</sup>	GO slim Biological Process	DMSO Control Cells: 	5µg/ml Benomyl Cells: 
(BY4741)	(WT)	NA	No			
YOR349W	CIN1	NA	Yes	cytoskeleton organization and biogenesis		
YER007W	PAC2	14.6	Yes	cytoskeleton organization and biogenesis		
YPL241C	CIN2	13.4	Yes	cytoskeleton organization and biogenesis		
YEL061C	CIN8	12.4	Yes	cell cycle		
YML124C	TUB3	9.5	Yes	meiosis		
YPL269W	KAR9	9.0	Yes	nuclear organization and biogenesis		
YEL003W	GIM4	8.7	No	cytoskeleton organization and biogenesis		
YER016W	BIM1	8.7	No	cytoskeleton organization and biogenesis		
YMR138W	CIN4	7.8	Yes	cytoskeleton organization and biogenesis		
YLR200W	YKE2	7.0	Yes	cytoskeleton organization and biogenesis		

YGL086W	MAD1	6.3	No	transport		
YOR265W	RBL2	6.1	No	protein binding		
YGL217C		6.1	No	unknown		
YJR053W	BFA1	6.0	No	conjugation		
YLR210W	CLB4	5.3	No	cell cycle		
YCL029C	BIK1	5.3	Yes	cell cycle		
YJL013C	MAD3	5.3	No	cell cycle		
YDR360W		5.2	No	unknown		
YOR058C	ASE1	4.7	No	cell cycle		
YPL008W	CHL1	4.6	No	cell cycle		
YMR055C	BUB2	4.6	No	cell cycle		
YGL216W	KIP3	4.6	Yes	cytoskeleton organization and biogenesis		
YBR107C	IML3	4.5	No	cell cycle		
YJL030W	MAD2	4.5	No	cell cycle		
YOR264W	DSE3	4.4	No	unknown		
YOR266W	PNT1	4.4	No	membrane organization and biogenesis		
YPL017C		4.4	No	unknown		
YGL124C	MON1	4.4	No	transport		
YOR026W	BUB3	4.3	Yes	cell cycle		
YLR381W	CTF3	4.0	No	cell cycle		
YJR135C	MCM22	4.0	No	cell cycle		

**Table S5.** The list of genes having average congruence score  $\geq 4$  with 7 benomyl-sensitive landmarks.

ORF name	Gene name	LD50 benomyl concentration (ug/ml)	Average congruence score with 7 landmarks	GO slim Biological Process
YML124C	TUB3	1	4	meiosis protein modification
YGR188C	BUB1	15	4	cell cycle
YJL030W	MAD2	20	4	cell cycle
YCL029C	BIK1	20	4	cytoskeleton organization and biogenesis
YPL241C	CIN2	5	5	transport
YGL086W	MAD1	20	5	cytoskeleton organization and biogenesis
YOR349W	CIN1	1	6	cytoskeleton organization and biogenesis
YLR200W	YKE2	5	8	cytoskeleton organization and biogenesis
YGR078C	PAC10	1	10	cytoskeleton organization and biogenesis
YNL153C	GIM3	1	11	cytoskeleton organization and biogenesis
YML094W	GIM5	1	12	cytoskeleton organization and biogenesis
YEL003W	GIM4	5	12	cytoskeleton organization and biogenesis

**Table S6.** The list of genes having  $\geq 4$  synthetic lethal interactions with 7 benomyl-sensitive landmarks.

ORF name	Gene name	LD50 benomyl concentration (ug/ml)	Number of synthetic lethal interactions with 7 landmarks	GO slim Biological Process
YML124C	TUB3	1	4	meiosis cytoskeleton organization and biogenesis
YOR349W	CIN1	1	4	organelle organization and biogenesis
YAL011W	SWC1	15	4	cell cycle
YJL030W	MAD2	20	4	cell cycle
YDR318W	MCM21	30	4	cell cycle
YCL016C	DCC1	30	4	cell cycle
YPL018W	CTF19	30	4	cell cycle
YHR191C	CTF8	35	4	cell cycle
YJL013C	MAD3	1	5	cell cycle cytoskeleton organization and biogenesis
YPL241C	CIN2	5	5	cytoskeleton organization and biogenesis
YMR138W	CIN4	10	5	protein binding
YOR265W	RBL2	20	5	transport
YGL086W	MAD1	20	5	cell cycle
YCL029C	BIK1	20	5	transcription
YOL012C	HTZ1	20	5	transport
YLR085C	ARP6	20	5	

**Table S7.** *PFD1* dSLAM targets. Genes exhibiting synthetic lethality in combination with *PFD1* were detected by microarray analysis after sporulation of a heterozygous deletion mutant pool that had been transformed with a *pdf1* knockout allele. The experimental (*pdf1 yko*): control (*yko*) tag signal ratios were determined from Uptag and Downtag hybridizations. In our experience, a signal ratio >2 for both tags represents a conservative criterion for identification of true synthetic lethal relationships (minimizing false positives). Protein complex residence of *PFD1* dSLAM targets is indicated by the name of the bait protein used to identify complex members.

ORF Name	Gene Name	log2(Ratio) Downtag	log2(Ratio) Uptag	Protein Complex Residence
YMR074C		4.71	3.99	
YOR349W	CIN1	5.35	3.93	CDC55 <sup>(Ho et al, 2002)</sup>
YDR334W	SWR1	3.70	5.12	
YML124C	TUB3	3.53	4.69	HIS4 <sup>(Gavin et al, 2002)</sup> , RAD3 <sup>(Gavin et al, 2002)</sup> , YDR060W <sup>(Gavin et al, 2002)</sup> , YLL013C <sup>(Gavin et al, 2002)</sup>
YPL241C	CIN2	3.59	3.19	
YOL012C	HTZ1	3.05	3.66	NAP1 <sup>(Gavin et al, 2002)</sup> , RAD16 <sup>(Ho et al, 2002)</sup>
YLR085C	ARP6	2.92	3.33	
YKL025C	PAN3	2.65	2.00	PAN2 <sup>(Gavin et al, 2002)</sup>
YNL054W	VAC7	1.91	2.48	
YOR073W	SGO1	1.81	2.85	BUD32 <sup>(Ho et al, 2002)</sup>
YCL029C	BIK1	2.22	1.73	LAP4 <sup>(Ho et al, 2002)</sup>
YML112W	CTK3	1.72	2.61	CTK1 <sup>(Gavin et al, 2002)</sup> , CTK3 <sup>(Ho et al, 2002)</sup>
YJL030W	MAD2	1.69	1.55	
YKL037W		1.31	1.60	
YCR009C	RVS161	1.29	1.80	RVS161 <sup>(Ho et al, 2002)</sup> , RVS167 <sup>(Ho et al, 2002)</sup> , SEC27 <sup>(Ho et al, 2002)</sup>
YBR231C	AOR1	1.24	3.47	
YPL174C	NIP100	1.22	1.34	
YNL148C	ALF1	1.21	2.88	
YER016W	BIM1	1.46	1.20	
YJL129C	TRK1	1.20	1.25	
YNL248C	RPA49	1.17	1.45	RPA190 <sup>(Gavin et al, 2002)</sup> , RPC40 <sup>(Gavin et al, 2002)</sup> , (Ho et al, 2002)
YNL296W	KRE25	1.41	1.17	
YNL273W	TOF1	1.16	1.26	
YER177W	BMH1	1.39	1.16	BMH1 <sup>(Ho et al, 2002)</sup> , BMH2 <sup>(Gavin et al, 2002)</sup> , LCB2 <sup>(Gavin et al, 2002)</sup> , SNF4 <sup>(Gavin et al, 2002)</sup>
YLR370C	ARC18	1.25	1.14	ARC18 <sup>(Gavin et al, 2002)</sup> , ARC40 <sup>(Ho et al, 2002)</sup> , ARP2 <sup>(Ho et al, 2002)</sup>
YBR036C	CSG2	1.33	1.13	
YCR024C		1.13	1.48	
YLR442C	SIR3	1.08	1.59	
YGL094C	PAN2	1.07	2.55	PAN2 <sup>(Gavin et al, 2002)</sup>
YER087W		1.20	1.03	
YNL086W		1.28	1.02	
YDL020C	RPN4	1.02	1.46	
YPR141C	KAR3	1.05	1.01	

YDR207C	UME6	1.01	1.76	YDL076C <sup>(Gavin et al, 2002)</sup>
---------	------	------	------	--

**Table S8.** Prefoldin Congruence SGA-SGA and dSLAM-SGA:  $i$ , Gene 1 SL interaction set size;  $j$ , Gene 2 interaction set size;  $k$ , interaction set overlap; *Score*,  $-\text{Log}_{10}(P)$ . The total number of target genes is 4700. Because we used conservative dSLAM criteria to identify interactions, only those mutants scored as synthetic lethal (not synthetic sick) from the SGA data were kept for the congruence score comparison.

Comparison	Gene 1	Gene 2	i	j	k	Score
<b>SGA-SGA</b>	GIM3	GIM4	66	50	36	60
	GIM3	GIM5	66	29	19	29
	GIM3	PAC10	66	72	43	67
	GIM3	YKE2	66	47	36	62
	GIM4	GIM5	50	29	16	25
	GIM4	PAC10	50	72	30	44
	GIM4	YKE2	50	47	26	42
	GIM5	PAC10	29	72	19	28
	GIM5	YKE2	29	47	15	23
	PAC10	YKE2	72	47	34	55
<b>dSLAM-SGA</b>	PFD1	GIM3	33	66	12	14
	PFD1	GIM4	33	50	11	14
	PFD1	GIM5	33	29	7	9
	PFD1	PAC10	33	72	13	15
	PFD1	YKE2	33	47	12	16

**Table S9.** The dSLAM screen results for query genes *LTE1*, *SPO12*, and *SLK19*. Every synthetic lethal interaction has been confirmed by either random spore analysis (RSA) or tetrad analysis.

Query ORF	Query Gene	Target ORF	Target Gene	RSA	TETRAD
YAL024C	LTE1	YAL013W	DEP1	SL	
YAL024C	LTE1	YAR003W	SWD1	SF	
YAL024C	LTE1	YBL016W	FUS3	SF	
YAL024C	LTE1	YBL025W	RRN10	SF	
YAL024C	LTE1	YBL031W	SHE1	SF	
YAL024C	LTE1	YBL032W	HEK2	SF	
YAL024C	LTE1	YBL058W	SHP1	SL	
YAL024C	LTE1	YBR036C	CSG2	SF	
YAL024C	LTE1	YBR058C	UBP14	SF/SL	
YAL024C	LTE1	YBR097W	VPS15	SF/SL	
YAL024C	LTE1	YBR119W	MUD1	SF/SL	
YAL024C	LTE1	YBR174C		SF	
YAL024C	LTE1	YBR175W	SWD3	SF	
YAL024C	LTE1	YBR200W	BEM1	SL	
YAL024C	LTE1	YBR267W		SF	
YAL024C	LTE1	YCL016C	DCC1	SL	
YAL024C	LTE1	YCL037C	SRO9	SF	
YAL024C	LTE1	YCL060C		SF	
YAL024C	LTE1	YCL061C	MRC1	SF	
YAL024C	LTE1	YCL063W	VAC17	SF	
YAL024C	LTE1	YCR016W		SF	
YAL024C	LTE1	YCR066W	RAD18	SF	
YAL024C	LTE1	YCR094W	CDC50	SF	
YAL024C	LTE1	YDL006W	PTC1	SF	
YAL024C	LTE1	YDL040C	NAT1	SF	
YAL024C	LTE1	YDL056W	MBP1	SF	
YAL024C	LTE1	YDL059C	RAD59	SF	
YAL024C	LTE1	YDL074C	BRE1	SF/SL	
YAL024C	LTE1	YDL090C	RAM1	SF	
YAL024C	LTE1	YDL115C	IWR1	SL	
YAL024C	LTE1	YDL130W	RPP1B	SF	
YAL024C	LTE1	YDL136W	RPL35B	SF	
YAL024C	LTE1	YDL144C		SF	
YAL024C	LTE1	YDL190C	UFD2	SF	
YAL024C	LTE1	YDL225W	SHS1	SF	
YAL024C	LTE1	YDL236W	PHO13	SF	
YAL024C	LTE1	YDR004W	RAD57	SF	
YAL024C	LTE1	YDR065W		SF	
YAL024C	LTE1	YDR071C		SF	



YAL024C	LTE1	YDR076W	RAD55	SF	
YAL024C	LTE1	YDR101C	ARX1	SF	
YAL024C	LTE1	YDR114C		SF	
YAL024C	LTE1	YDR117C		SF	
YAL024C	LTE1	YDR121W	DPB4	SF	
YAL024C	LTE1	YDR146C	SWI5	SF	
YAL024C	LTE1	YDR149C		SF	
YAL024C	LTE1	YDR150W	NUM1	SF	
YAL024C	LTE1	YDR159W	SAC3	SL	
YAL024C	LTE1	YDR174W	HMO1	SF	
YAL024C	LTE1	YDR200C	VPS64	SF	
YAL024C	LTE1	YDR207C	UME6	SL	
YAL024C	LTE1	YDR260C	SWM1	SF/SL	
YAL024C	LTE1	YDR310C	SUM1	SL	
YAL024C	LTE1	YDR359C	VID21	SF	
YAL024C	LTE1	YDR369C	XRS2	SF	
YAL024C	LTE1	YDR392W	SPT3	SF/SL	
YAL024C	LTE1	YDR432W	NPL3	SL	
YAL024C	LTE1	YDR463W	STP1	SF	
YAL024C	LTE1	YDR469W	SDC1	SF	
YAL024C	LTE1	YDR497C	ITR1	SF/SL	
YAL024C	LTE1	YDR532C		SL	
YAL024C	LTE1	YEL029C	BUD16	SF	
YAL024C	LTE1	YEL031W	SPF1	SF	
YAL024C	LTE1	YEL037C	RAD23	SF	
YAL024C	LTE1	YEL054C	RPL12A	SF	
YAL024C	LTE1	YEL061C	CIN8	SF	
YAL024C	LTE1	YEL062W	NPR2	SF	
YAL024C	LTE1	YER014W	HEM14	SF	
YAL024C	LTE1	YER016W	BIM	SL	
YAL024C	LTE1	YER073W	ALD5	SL	
YAL024C	LTE1	YER095W	RAD51	SF	
YAL024C	LTE1	YER110C	KAP123	SF	
YAL024C	LTE1	YER123W	YCK3	SF	
YAL024C	LTE1	YER139C		SF	
YAL024C	LTE1	YFR036W	CDC26	SF	
YAL024C	LTE1	YGL045W	RIM8	SF	
YAL024C	LTE1	YGL060W		SF	
YAL024C	LTE1	YGL066W	SGF73	SL	
YAL024C	LTE1	YGL072C		SL	
YAL024C	LTE1	YGL078C	DBP3	SF	
YAL024C	LTE1	YGL127C	SOH1	SF/SL	

YAL024C	LTE1	YGL133W	ITC1	SF/SL	
YAL024C	LTE1	YGL163C	RAD54	SF	
YAL024C	LTE1	YGL167C	PMR1	SF	
YAL024C	LTE1	YGL228W	SHE10	SF	
YAL024C	LTE1	YGR046W		SF	
YAL024C	LTE1	YGR056W	RSC1	SF	
YAL024C	LTE1	YGR077C	PEX8	SF	
YAL024C	LTE1	YGR078C	PAC10	SF	
YAL024C	LTE1	YGR134W	CAF130	SF	
YAL024C	LTE1	YGR180C	RNR4	SL	
YAL024C	LTE1	YGR192C	TDH3	SF/SL	
YAL024C	LTE1	YGR260W	TNA1	SF	
YAL024C	LTE1	YHL007C	STE20	SL	
YAL024C	LTE1	YHL027W	RIM101	SF	
YAL024C	LTE1	YHL033C	RPL8A	SF/SL	
YAL024C	LTE1	YHR013C	ARD1	SF	
YAL024C	LTE1	YHR031C	RRM3	SF	
YAL024C	LTE1	YHR034C		SF	
YAL024C	LTE1	YHR041C	SRB2	SL	
YAL024C	LTE1	YHR067W	RMD12	SF	
YAL024C	LTE1	YHR100C		SF	
YAL024C	LTE1	YHR129C	ARP1	SF	
YAL024C	LTE1	YHR152W	SPO12	SL	
YAL024C	LTE1	YHR154W	RTT107	SF	
YAL024C	LTE1	YHR178W	STB5	SL	
YAL024C	LTE1	YHR191C	CTF8	SL	
YAL024C	LTE1	YHR200W	RPN10	SL	
YAL024C	LTE1	YIL036W	CST6	SF	
YAL024C	LTE1	YIL084C	SDS3	SL	
YAL024C	LTE1	YIL103W		SF	
YAL024C	LTE1	YIR023W	DAL81	SF	
YAL024C	LTE1	YIR033W	MGA2	SF	
YAL024C	LTE1	YJL047C	RTT101	SF	
YAL024C	LTE1	YJL080C	SCP160	SL	
YAL024C	LTE1	YJL098W	SAP185	SF	
YAL024C	LTE1	YJL115W	ASF1	SF/SL	
YAL024C	LTE1	YJL120W		SF	
YAL024C	LTE1	YJL121C	RPE1	SF	
YAL024C	LTE1	YJL128C	PBS2	SF	
YAL024C	LTE1	YJL148W	RPA34	SF	
YAL024C	LTE1	YJL177W	RPL17B	SF	
YAL024C	LTE1	YJL179W	PFD1	SF	

YAL024C	LTE1	YJR043C	POL32	SF	
YAL024C	LTE1	YJR050W	ISY1	SF	
YAL024C	LTE1	YJR055W	HIT1	SL	
YAL024C	LTE1	YJR055W	HIT1	SF	
YAL024C	LTE1	YJR074W	MOG1	SL	
YAL024C	LTE1	YJR097W		SF	
YAL024C	LTE1	YJR102C	VPS25	SF	
YAL024C	LTE1	YKL006W	RPL14A	SL	
YAL024C	LTE1	YKL053W		SF	
YAL024C	LTE1	YKL074C	MUD2	SF	
YAL024C	LTE1	YKL113C	RAD27	SF	
YAL024C	LTE1	YKR047W		SF	
YAL024C	LTE1	YKR048C	NAP1	SF	
YAL024C	LTE1	YKR054C	DYN1	SF	
YAL024C	LTE1	YKR061W	KTR2	SL	
YAL024C	LTE1	YKR073C		SF	
YAL024C	LTE1	YKR092C	SRP40	SF	
YAL024C	LTE1	YLL002W	RTT109	SF	
YAL024C	LTE1	YLL049W		SF	
YAL024C	LTE1	YLR015W	BRE2	SF	
YAL024C	LTE1	YLR027C	AAT2	SL	
YAL024C	LTE1	YLR032W	RAD5	SF	
YAL024C	LTE1	YLR055C	SPT8	SL	
YAL024C	LTE1	YLR067C	PET309	SF	
YAL024C	LTE1	YLR079W	SIC1	SF	
YAL024C	LTE1	YLR102C	APC9	SL	
YAL024C	LTE1	YLR200W	YKE2	SF	
YAL024C	LTE1	YLR204W	QRI5	SF	
YAL024C	LTE1	YLR234W	TOP3	SL	
YAL024C	LTE1	YLR235C		SL	
YAL024C	LTE1	YLR240W	VPS34	SF	
YAL024C	LTE1	YLR315W	NKP2	SF	
YAL024C	LTE1	YLR320W	MMS22	SL	
YAL024C	LTE1	YLR338W		SL	
YAL024C	LTE1	YLR357W	RSC2	SL	
YAL024C	LTE1	YLR358C		SL	
YAL024C	LTE1	YLR370C	ARC18	SL	
YAL024C	LTE1	YLR373C	VID22	SF	
YAL024C	LTE1	YLR374C		SF	
YAL024C	LTE1	YLR386W	VAC14	SF	
YAL024C	LTE1	YLR406C	RPL31B	SF	
YAL024C	LTE1	YLR410W	VIP1	SL	

YAL024C	LTE1	YLR417W	VPS36	SF	
YAL024C	LTE1	YLR448W	RPL6B	SF/SL	
YAL024C	LTE1	YML032C	RAD52	SF	
YAL024C	LTE1	YML036W		SL	
YAL024C	LTE1	YML061C	PIF1	SF	
YAL024C	LTE1	YML094W	GIM5	SF	
YAL024C	LTE1	YML103C	NUP188	SF	
YAL024C	LTE1	YML128C	MSC1	SF/SL	
YAL024C	LTE1	YMR022W	QRI8	SF	
YAL024C	LTE1	YMR039C	SUB1	SF	
YAL024C	LTE1	YMR048W	CSM3	SF	
YAL024C	LTE1	YMR063W	RIM9	SF	
YAL024C	LTE1	YMR078C	CTF18	SL	
YAL024C	LTE1	YMR144W		SF	
YAL024C	LTE1	YMR154C	RIM13	SF	
YAL024C	LTE1	YMR165C	SMP2	SL	
YAL024C	LTE1	YMR179W	SPT21	SL	
YAL024C	LTE1	YMR194W	RPL36A	SF	
YAL024C	LTE1	YMR198W	CIK1	SF/SL	
YAL024C	LTE1	YMR198W	CIK1	SL	
YAL024C	LTE1	YMR205C	PFK2	SL	
YAL024C	LTE1	YMR214W	SCJ1	SF	
YAL024C	LTE1	YMR224C	MRE11	SF	
YAL024C	LTE1	YMR261C	TPS3	SF	
YAL024C	LTE1	YMR263W	SAP30	SL	
YAL024C	LTE1	YMR267W	PPA2	SF	
YAL024C	LTE1	YMR269W		SF	
YAL024C	LTE1	YMR274C	RCE1	SF	
YAL024C	LTE1	YMR294W	JNM1	SF	
YAL024C	LTE1	YMR299C		SF	
YAL024C	LTE1	YNL054W	VAC7	SF/SL	
YAL024C	LTE1	YNL064C	YDJ1	SL	
YAL024C	LTE1	YNL068C	FKH2	SF	
YAL024C	LTE1	YNL076W	MKS1	SF/SL	
YAL024C	LTE1	YNL084C	END3	SF/SL	
YAL024C	LTE1	YNL097C	PHO23	SL	
YAL024C	LTE1	YNL147W	LSM7	SF/SL	
YAL024C	LTE1	YNL148C	ALF1	SF	
YAL024C	LTE1	YNL153C	GIM3	SF	
YAL024C	LTE1	YNL171C		SL	
YAL024C	LTE1	YNL198C		SF	
YAL024C	LTE1	YNL199C	GCR2	SL	

YAL024C	LTE1	YNL229C	URE2	SF	
YAL024C	LTE1	YNL236W	SIN4	SF	
YAL024C	LTE1	YNL250W	RAD50	SF	
YAL024C	LTE1	YNL273W	TOF1	SF	
YAL024C	LTE1	YNL294C	RIM21	SL	
YAL024C	LTE1	YNL330C	RPD3	SL	
YAL024C	LTE1	YNR009W		SF	
YAL024C	LTE1	YOL004W	SIN3	SL	
YAL024C	LTE1	YOL041C	NOP12	SF/SL	
YAL024C	LTE1	YOL068C	HST1	SF	
YAL024C	LTE1	YOR035C	SHE4	SF	
YAL024C	LTE1	YOR080W	DIA2	SL	
YAL024C	LTE1	YOR082C		SF	
YAL024C	LTE1	YOR083W	WHI5	SF	
YAL024C	LTE1	YOR195W	SLK19	SL	
YAL024C	LTE1	YOR209C	NPT1	SL	
YAL024C	LTE1	YOR211C	MGM1	SL	
YAL024C	LTE1	YOR221C	MCT1	SF	
YAL024C	LTE1	YOR271C		SF	
YAL024C	LTE1	YOR275C	RIM20	SF	
YAL024C	LTE1	YOR295W	UAF30	SL	
YAL024C	LTE1	YOR297C	TIM18	SF	
YAL024C	LTE1	YOR304W	ISW2	SL	
YAL024C	LTE1	YOR344C	TYE7	SF	
YAL024C	LTE1	YOR360C	PDE2	SF	
YAL024C	LTE1	YPL008W	CHL1	SF	
YAL024C	LTE1	YPL055C	LGE1	SF	
YAL024C	LTE1	YPL059W	GRX5	SF	
YAL024C	LTE1	YPL080C		SF	
YAL024C	LTE1	YPL084W	BRO1	SL	
YAL024C	LTE1	YPL106C	SSE1	SF	
YAL024C	LTE1	YPL139C	UME1	SF	
YAL024C	LTE1	YPL161C	BEM4	SL	
YAL024C	LTE1	YPL174C	NIP100	SF	
YAL024C	LTE1	YPL178W	CBC2	SF	
YAL024C	LTE1	YPL182C		SF	
YAL024C	LTE1	YPL184C		SF	
YAL024C	LTE1	YPL188W	POS5	SL	
YAL024C	LTE1	YPL213W	LEA1	SF	
YAL024C	LTE1	YPL269W	KAR9	SF	
YAL024C	LTE1	YPR029C	APL4	SF	
YAL024C	LTE1	YPR054W	SMK1	SF	

YAL024C	LTE1	YPR119W	CLB2	SF	
YAL024C	LTE1	YPR135W	CTF4	SL	
YAL024C	LTE1	YPR141C	KAR3	SF	
YHR152W	SPO12	YAL024C	LTE1		SL
YHR152W	SPO12	YGL003C	CDH1		SL
YHR152W	SPO12	YNL171C			SL
YHR152W	SPO12	YNL225C	CNM67		SL
YHR152W	SPO12	YNL298W	CLA4		SL
YOR195W	SLK19	YAL024C	LTE1		SL
YOR195W	SLK19	YCR086W	CSM1		SF
YOR195W	SLK19	YDR200C	VPS64		SL
YOR195W	SLK19	YDR359C	VID21		SL
YOR195W	SLK19	YDR439W	LRS4		SL
YOR195W	SLK19	YEL061C	CIN8		SL
YOR195W	SLK19	YER016W	BIM1		SL
YOR195W	SLK19	YGL003C	CDH1		SL
YOR195W	SLK19	YGR188C	BUB1		SL
YOR195W	SLK19	YHR191C	CTF8		SF
YOR195W	SLK19	YJL124C	LSM1		SL
YOR195W	SLK19	YKL057C	NUP120		SL
YOR195W	SLK19	YKR082W	NUP133		SL
YOR195W	SLK19	YML112W	CTK3		SL
YOR195W	SLK19	YMR078C	CTF18		SL
YOR195W	SLK19	YMR198W	CIK1		SL
YOR195W	SLK19	YNL225C	CNM67		SL
YOR195W	SLK19	YNL298W	CLA4		SL
YOR195W	SLK19	YOR026W	BUB3		SL

**Table S10.** Congruence scores for FEAR and MEN pathway members:  $i$ , Gene 1 SL interaction set size;  $j$ , Gene 2 interaction set size;  $k$ , interaction set overlap; Score,  $-\text{Log}_{10}$  (hypergeometric  $P$ -value). The total number of target genes is 4700.

Comparison	Gene 1	Gene 2	$i$	$j$	$k$	Score
<b>dSLAM-dSLAM</b>	SPO12	SLK19	5	19	4	9
	SPO12	LTE1	5	252	1	1
	SLK19	LTE1	19	252	7	4
<b>dSLAM-SGA</b>	CLA4	LTE1	67	252	31	22
	CLA4	SPO12	67	5	0	0
	CLA4	SLK19	67	19	2	2

## References

- Ashburner M, Ball CA, Blake JA, Botstein D, Butler H, Cherry JM, Davis AP, Dolinski K, Dwight SS, Eppig JT, Harris MA, Hill DP, Issel-Tarver L, Kasarskis A, Lewis S, Matese JC, Richardson JE, Ringwald M, Rubin GM and Sherlock G (2000) Gene ontology: tool for the unification of biology. The Gene Ontology Consortium. *Nat Genet* **25**: 25-29
- Gavin AC, Bosche M, Krause R, Grandi P, Marzioch M, Bauer A, Schultz J, Rick JM, Michon AM, Cruciat CM, Remor M, Hofert C, Schelder M, Brajenovic M, Ruffner H, Merino A, Klein K, Hudak M, Dickson D, Rudi T et al (2002) Functional organization of the yeast proteome by systematic analysis of protein complexes. *Nature* **415**: 141-147
- Geissler S, Siegers K and Schiebel E (1998) A novel protein complex promoting formation of functional alpha- and gamma-tubulin. *Embo J* **17**: 952-966
- Ho Y, Gruhler A, Heilbut A, Bader GD, Moore L, Adams SL, Millar A, Taylor P, Bennett K, Boutilier K, Yang L, Wolting C, Donaldson I, Schandorff S, Shewnarane J, Vo M, Taggart J, Goudreault M, Muskut B, Alfarano C et al (2002) Systematic identification of protein complexes in *Saccharomyces cerevisiae* by mass spectrometry. *Nature* **415**: 180-183
- Ito T, Chiba T, Ozawa R, Yoshida M, Hattori M and Sakaki Y (2001) A comprehensive two-hybrid analysis to explore the yeast protein interactome. *Proc Natl Acad Sci U S A* **98**: 4569-4574
- James P, Halladay J and Craig EA (1996) Genomic libraries and a host strain designed for highly efficient two-hybrid selection in yeast. *Genetics* **144**: 1425-1436
- Lord PW, Stevens RD, Brass A and Goble CA (2003) Investigating semantic similarity measures across the Gene Ontology: the relationship between sequence and annotation. *Bioinformatics* **19**: 1275-1283
- Mewes HW, Amid C, Arnold R, Frishman D, Guldener U, Mannhaupt G, Munsterkotter M, Pagel P, Strack N, Stumpflen V, Warfsmann J and Ruepp A (2004) MIPS: analysis and annotation of proteins from whole genomes. *Nucleic Acids Res* **32 Database issue**: D41-44
- Tong AH, Lesage G, Bader GD, Ding H, Xu H, Xin X, Young J, Berriz GF, Brost RL, Chang M, Chen Y, Cheng X, Chua G, Friesen H, Goldberg DS, Haynes J, Humphries C, He G, Hussein S, Ke L et al (2004) Global mapping of the yeast genetic interaction network. *Science* **303**: 808-813



Uetz P, Giot L, Cagney G, Mansfield TA, Judson RS, Knight JR, Lockshon D, Narayan V, Srinivasan M, Pochart P, Qureshi-Emili A, Li Y, Godwin B, Conover D, Kalbfleisch T, Vijayadamodar G, Yang M, Johnston M, Fields S and Rothberg JM (2000) A comprehensive analysis of protein-protein interactions in *Saccharomyces cerevisiae*. *Nature* **403**: 623-627

Vainberg IE, Lewis SA, Rommelaere H, Ampe C, Vandekerckhove J, Klein HL and Cowan NJ (1998) Prefoldin, a chaperone that delivers unfolded proteins to cytosolic chaperonin. *Cell* **93**: 863-873

Wong SL, Zhang LV, Tong AH, Li Z, Goldberg DS, King OD, Lesage G, Vidal M, Andrews B, Bussey H, Boone C and Roth FP (2004) Combining biological networks to predict genetic interactions. *Proc Natl Acad Sci U S A* **101**: 15682-15687